Relativistic calculations of x-ray emission following a Xe-Bi^{83+} collision

Y. S. Kozhedub,[1,2] V. M. Shabaev,[1] I. I. Tupitsyn,[1] A. Gumberidze,[3] S. Hagmann,[3] G. Plunien,[4] and Th. Stöhlker[3,5]

[1]*Department of Physics, St. Petersburg State University, Ulianovskaya 1, Petrodvorets, St. Petersburg 198504, Russia*

[2]*SSC RF ITEP of NRC "Kurchatov Institute", Bolshaya Cheremushkinskaya 25, Moscow, 117218, Russia*

[3]*GSI Helmholtzzentrum für Schwerionenforschung, D-64291 Darmstadt, Germany*

[4]*Institut für Theoretische Physik, Technische Universität Dresden, Mommsenstraße 13, D-01062 Dresden, Germany*

[5]*Helmholtz-Institut Jena, D-07743 Jena, Germany*

(Received 30 August 2014; published 17 October 2014)

We study the x-ray emission following the collision of a Bi^{83+} ion with a neutral Xe atom at the projectile energy 70 MeV/u. The collisional and post-collisional processes are treated separately. The probabilities of various many-electron processes at the collision are calculated within a relativistic independent electron model using the coupled-channel approach with atomiclike Dirac-Fock-Sturm orbitals. The analysis of the post-collisional processes resulting in the x-ray emission is based on the fluorescence yields, the radiation, and Auger decay rates, and allows one to derive intensities of the x-ray emission and compare them with experimental data. A reasonable agreement between the theoretical results and the recent experimental data is observed. The role of the relativistic effects is investigated.

DOI: 10.1103/PhysRevA.90.042709 PACS number(s): 34.10.+x, 34.50.−s, 34.70.+e

I. INTRODUCTION

Collisions between multiply charged ions and atoms have been a subject of intensive studies for many years. Depending on the number of active electrons in the target atom and the charge state of the projectile, the multiple electronic ionization, excitation, and capture are possible, and multiple excited states can be formed. These states decay by emission of photons and/or electrons (Auger decay), both carrying information on the collision dynamics.

A significant progress in describing the quantum dynamics of electrons in low-energy ion-atom collisions has been made by studying various collision systems experimentally and theoretically (see Refs. [1–14] and references therein). The results are especially successful for low-Z (Z is the nuclear charge number) atoms and ions with a small number of active electrons. However, for collisions between highly charged ions (HCI) and heavy targets, both experimental data and theoretical analyses are scarce due to the complex nature of the problem. Meanwhile collisions of HCI provide a unique tool for tests of relativistic and quantum electrodynamics (QED) effects in the scattering processes [15–17]. Investigations of such processes can also give an access to QED in supercritical fields, provided the total charge of the colliding nuclei is larger than the critical one, $Z_c = 173$ (see, e.g., Ref. [18] and references therein).

Experimental investigations aimed at the comprehensive study of various processes in low-energy heavy ion-atom collisions are anticipated at GSI and FAIR facilities (Darmstadt, Germany) [19–23]. In a recent experiment [24], the intensities of the post-collisional x-ray emissions have been resolved for collisions of Bi^{83+} ions with Xe target atoms at the projectile energy 70 MeV/u. These experiments require the corresponding theoretical calculations. In the present paper, we perform a relativistic quantum-mechanical calculation of the Bi^{83+}-Xe collision within an independent electron model using the coupled-channel approach with atomiclike Dirac-Fock-Sturm orbitals [25,26]. The post-collision decay analysis allows us to derive the x-ray radiation intensities and compare them with the experimental data. We also study the role of the relativistic effects.

The paper is organized as follows. In Sec. II A, the theoretical approach used to calculate the collision dynamics is briefly described. Section II B is devoted to the description of post-collision processes coming to the x-ray radiation. In Sec. III A, the results for the single and multiple electronic dynamic probabilities are given, while in Sec. III B the theoretical x-ray intensities are presented and compared with the experimental data. Some general remarks and comments are given in the last section.

Throughout the paper atomic units ($\hbar = e = m_e = 1$) are used.

II. THEORY

We consider the collision of a bare bismuth (Bi^{83+}) with a target xenon atom at the projectile energy $E = 70$ MeV/u. At this energy the ionization of the target is the dominant process, but the target excitation and the electron capture by the projectile ion are also possible. The excited xenon and bismuth ions decay via Auger processes or radiatively. In any case, the de-excitation processes (Auger or radiative decays) take much more time than the electronic dynamic processes during the collision. Therefore, the collisional and the post-collisional decay dynamics can be viewed as being independent from each other and thus we can treat them separately. For the collision part, we solve the time-dependent Dirac equation within the semiclassical approximation and an independent electron model. The corresponding theory is presented in Sec. II A. In Sec. II B, the x-ray radiation intensities for the post-collision part are evaluated using an analysis based on the fluorescence yields, the radiation, and Auger decay rates.

A. Collision

The ion-atom collision is considered in the semiclassical approximation, where the atomic nuclei move along the classical trajectories. The nuclei are considered as sources

of a time-dependent external potential, whereas the electrons are treated quantum mechanically. The many-electron time-dependent Dirac equation is considered in the framework of an independent particle model, in which the many-particle Hamiltonian $\hat{H}$ is approximated by a sum of single-particle Hamiltonians, $\hat{H}^{\rm eff} = \sum_i \hat{h}_i^{\rm eff}$, reducing the many-electron problem to a set of single-particle Dirac equations:

$$i\frac{\partial \psi_i(t)}{\partial t} = \hat{h}_i^{\rm eff}(t)\,\psi_i(t) \quad \text{with} \quad i = 1,\ldots,N, \tag{1}$$

where the wave functions $\psi_i(t)$ have to satisfy the initial conditions for the N electrons:

$$\lim_{t\to-\infty}(\psi_i(t) - \psi_i^0(t)) = 0 \quad \text{with} \quad i = 1,\ldots,N. \tag{2}$$

The many-electron wave function is given by a Slater determinant made up from the single-particle wave functions. The two-center Dirac-Kohn-Sham Hamiltonian is used for $\hat{h}^{\rm eff}$:

$$\hat{h}^{\rm eff} = c(\boldsymbol{\alpha}\cdot\boldsymbol{p}) + \beta c^2 + V_{\rm nucl}^A(\boldsymbol{r}_A) + V_{\rm nucl}^B(\boldsymbol{r}_B) + V_{\rm C}[\rho] + V_{\rm xc}[\rho], \tag{3}$$

where c is the speed of light and $\boldsymbol{\alpha}$, β are the Dirac matrices. $V_{\rm nucl}^{\alpha}(\boldsymbol{r}_\alpha)$ and $V_{\rm C}[\rho] = \int d^3\boldsymbol{r}'\,\frac{\rho(\boldsymbol{r}')}{|\boldsymbol{r}-\boldsymbol{r}'|}$ are the electron-nucleus interaction and the electron-electron Coulomb repulsion potentials, respectively, and $\rho(\boldsymbol{r})$ is the electron density of the system. The exchange-correlation potential $V_{\rm xc}[\rho]$ was taken in the Perdew-Zunger parametrization [27] including the self-interaction correction.

To solve Eq. (1) we use the coupled-channel approach with atomiclike Dirac-Fock-Sturm orbitals $\varphi_{\alpha,a}$ [25,28], localized at the ions (atoms). The time-dependent single-particle wave function $\psi_i(t)$ is represented as

$$\psi_i(\boldsymbol{r},t) = \sum_{\alpha=A,B}\sum_a C_{\alpha,a}^i(t)\,\varphi_{\alpha,a}(\boldsymbol{r}_\alpha(t)). \tag{4}$$

Here index $\alpha = A,B$ labels the centers, index a enumerates basis functions at the given center, $\boldsymbol{r}_\alpha = \boldsymbol{r} - \boldsymbol{R}_\alpha$, and $\varphi_{\alpha,a}(r_\alpha)$ is the central-field bispinor centered at the point α. The insertion of the expansion (4) into the Dirac-Kohn-Sham Eq. (1) leads to the well-known coupled-channel equations for the coefficients $C_{\alpha,a}^i(t)$,

$$i\sum_{\beta,b}\langle\varphi_{\beta,b}|\varphi_{\alpha,a}\rangle\frac{dC_{\beta,b}^i(t)}{dt} = \sum_{\beta,b}\langle\varphi_{\alpha,a}|\left(\hat{h}_i^{\rm eff} - i\frac{\partial}{\partial t}\right)|\varphi_{\beta,b}\rangle\,C_{\beta,b}^i(t), \tag{5}$$

where indices α,a and β,b enumerate the basis functions of both centers.

The expansion coefficients are determined employing the direct evolution (exponential) operator method [29], which is more stable compared to the others, such as, e.g., the Crank-Nicholsen propagation scheme [30] and the split-operator method [31]. To obtain the matrix representation of the exponential operator in the finite basis set one has to diagonalize the generalized complex Hamiltonian matrix at each time step. Since our basis set is not too large, the diagonalization procedure is not too time consuming.

The transition probability from a given initial configuration of colliding ions $(i_1,\ldots,i_N)$ to a given final configuration $(f_1,\ldots,f_N)$ is defined by

$$P_{f_1,\ldots,f_N} = |\langle f_1,\ldots,f_N|i_1,\ldots,i_N;t_f\rangle|^2. \tag{6}$$

Here, $|i_1,\ldots,i_N;t\rangle$ denotes the Slater determinant constructed from the solutions of the effective one-particle Eq. (1) at time t for the initial condition $(i_1,\ldots,i_N)$. The probability can be written as the $(N\times N)$ determinant of the one-particle density matrix [32,33],

$$P_{f_1,\ldots,f_N} = \det(\gamma_{nn'}), \quad n,n' = 1,\ldots,N, \tag{7}$$

where

$$\gamma_{nn'} = \langle f_n|\left[\sum_{i=1}^N|\psi_i(x,t=\infty)\rangle\langle\psi_i(x',t=\infty)|\right]|f_{n'}\rangle. \tag{8}$$

The probability to find q electrons in given states is determined by formulas,

$$P_{f_1,\ldots,f_q} = \sum_{f_{q+1}<\cdots<f_N} P_{f_1,\ldots,f_N}, \quad q < N, \tag{9}$$

$$P_{f_1,\ldots,f_q} = \det(\gamma_{nn'}), \quad n,n' = 1,\ldots,q, \quad q < N. \tag{10}$$

The corresponding inclusive probability for a configuration with q occupancies and $L-q$ holes, in terms of inclusive probabilities related only to occupancies, takes the form,

$$P_{f_1,\ldots,f_q}^{f_{q+1},\ldots,f_L} = P_{f_1,\ldots,f_q} - \sum_{f_{q+1}} P_{f_1,\ldots,f_q,f_{q+1}} + \sum_{f_{q+1}<f_{q+2}} P_{f_1,\ldots,f_q,f_{q+1},f_{q+2}} + \cdots + (-1)^{L-q}P_{f_1,\ldots,f_q,f_{q+1},\ldots,f_L}. \tag{11}$$

B. X-ray radiation

In order to evaluate the intensities of the K and L x-ray radiation of the ions after the collision we use a scheme, the main steps of which are the following:

(1) to look for states f of the ions which can de-excite via the considered x-ray radiation;

(2) to calculate the probabilities P_f to find the system in the states f after the collision;

(3) to determine the radiative de-excitation probabilities with m emitted x-ray photons for the states f under consideration, $P_m^{\rm rad}(f)$;

(4) to evaluate the "relative" x-ray radiation intensities (the number of the emitted photons per collision) as $I = \sum_f m P_m^{\rm rad}(f) P_f$.

The values P_f are derived as described in Sec. II A. To determine the values of $P_m^{\rm rad}(f)$ we are guided by the fluorescence yield, the radiation, and Auger decay rates, and some features of the ion states f.

As a brief example, let us consider the K x-ray radiation of the xenon ion following the collision. The K radiation is possible for states having the K-shell vacancies. Actually there are two different cases: the states with only one and the states with exactly two K-shell vacancies. These states are filled through the radiative de-excitation, which probability is defined by the fluorescence yield coefficient for the xenon K

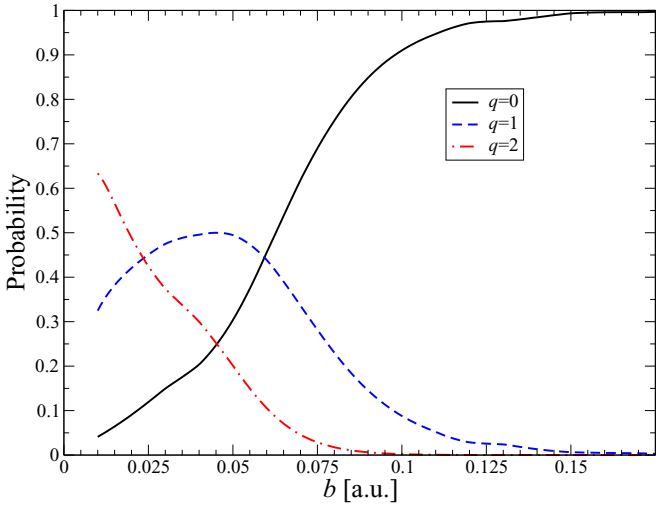

FIG. 1. (Color online) The probabilities of the Xe q-K-shell-vacancy production in the Xe-Bi^{83+} collision as functions of the impact parameter b.

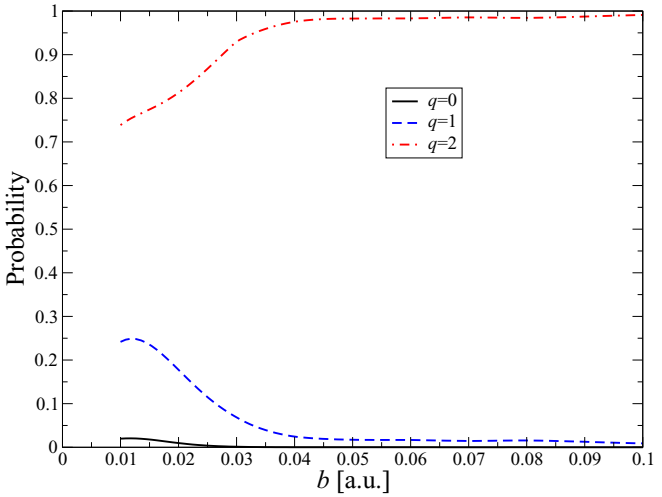

FIG. 3. (Color online) The probabilities of the Bi q-K-shell-vacancy surviving in the Xe-Bi^{83+} collision as functions of the impact parameter b.

shell $P^{\rm rad}(K)$ (it is assumed that the higher energy shells are occupied rather densely). If P_1 and P_2 are the probabilities to find one and two K-shell vacancies, the relative K x-ray radiation intensity is $I_K = P^{\rm rad}(K)(P_1 + 2P_2)$.

III. RESULTS OF THE CALCULATIONS AND DISCUSSION

A. Collision

The method described in Sec. II A was applied to the Xe and Bi^{83+} collision at the projectile energy 70 keV/u. Since we are interested in the K and L x-ray radiation of the ions, we focus first on the study of the K- and L-shell electronic population probabilities for the colliding ions.

Figures 1 and 2 show the probabilities of the q-vacancies creation in the K and L shells of the target ion (xenon), correspondingly, as functions of the impact parameter. We note that the probability of the K-shell-vacancy production becomes significant for the impact parameter b less than 0.1 a.u. and for $b < 0.06$ a.u. this probability is dominating (the size of the K shell is about 0.02 a.u.). When the impact parameter is close to zero, the probability to find at least one electron in the K shell is almost vanishing.

As one can see from Fig. 2, the results for the L-shell-vacancy production probabilities are similar to the K-shell ones. The L-shell electron loss probability grows rapidly when the impact parameter b becomes smaller than 0.5 a.u. (the size of the L shell is about 0.1 a.u.). At $b < 0.3$ a.u. the vacancy creation is the dominant process and, moreover, at $b < 0.2$ a.u. the multiple vacancy production mainly takes place.

The results of the calculations for the post-collisional bismuth states are presented in Figs. 3–6. Figure 3 displays that the K shell of bismuth is almost empty for a wide range of

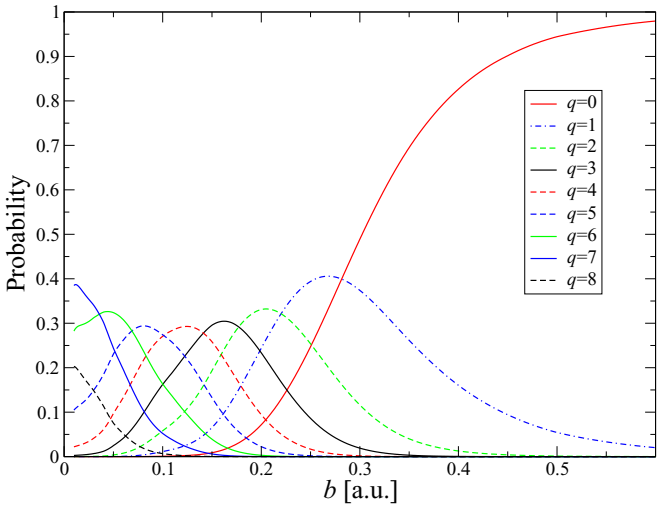

FIG. 2. (Color online) The probabilities of the Xe q-L-shell-vacancy production in the Xe-Bi^{83+} collision as functions of the impact parameter b.

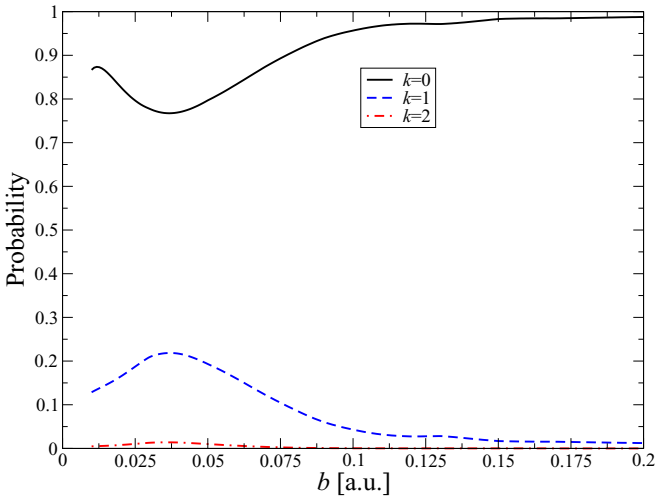

FIG. 4. (Color online) The probabilities of the Bi k-L_1-shell ($2s$) electronic population in the Xe-Bi^{83+} collision as functions of the impact parameter b.

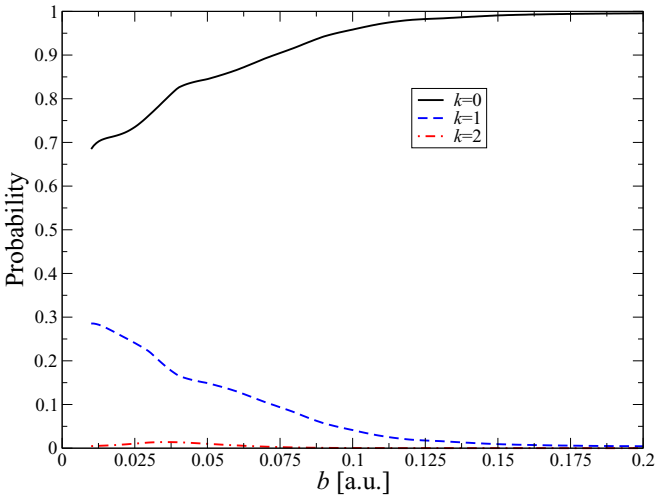

FIG. 5. (Color online) The probabilities of the Bi k-L_2-shell ($2p_{1/2}$) electronic population in the Xe-Bi^{83+} collision as functions of the impact parameter b.

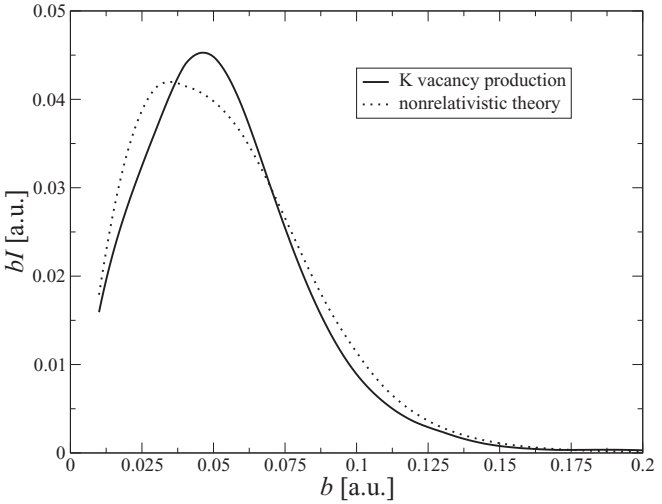

FIG. 7. The intensity I of the Xe K-shell-vacancy production weighted by the impact parameter in the Xe-Bi^{83+} collision as a function of the impact parameter b. The dotted line indicates the results of the nonrelativistic calculations.

the impact parameter value. The maximum of the probability to observe at least one electron in the K shell achieves 0.25 at $b = 0.012$ a.u. (the size of the K shell is about 0.016 a.u.).

The L bismuth shells are conveniently described in terms of electronic population probabilities. The k-L-shell electronic population probabilities for the L_1 ($2s$), L_2 ($2p_{1/2}$), L_3 ($2p_{3/2}$) shells as functions of the impact parameter are presented in Figs. 4, 5, and 6, respectively. The probabilities are not large and we can conclude that the probability to find more than two electrons at the L shell is almost zero.

B. X-ray radiation

After the collision the xenon atom (target) is generally a highly ionized and excited ion with a large number of the K- and L-shell vacancies. Nevertheless, the binding electrons are in plenty and during de-excitation processes all the K- and L-shell vacancies are filled by electrons with the emission of the K and L x-ray photons in accordance with the fluorescence yield probabilities $P^{\rm rad}(K)$ and $P^{\rm rad}(L)$, correspondingly. Let $I_K(b) = \sum_q q P_{K,q}(b)$ is the intensity of the K-shell-vacancy production per collision as a function of the impact parameter b. Here $P_{K,q}(b)$ is the probability of the q-K-shell-vacancy production. Then the intensities of the K and L x-ray radiation are given by

$$I_K^{\rm rad} = 2\pi P^{\rm rad}(K) \int_0^\infty I_K(b) b db, \tag{12}$$

$$I_L^{\rm rad} = 2\pi P^{\rm rad}(L) \int_0^\infty I_L(b) b db. \tag{13}$$

The results of the calculations for $I_K(b)$ and $I_L(b)$ weighted by the impact parameter are presented in Figs. 7 and 8, respectively. To investigate the role of the relativistic effects

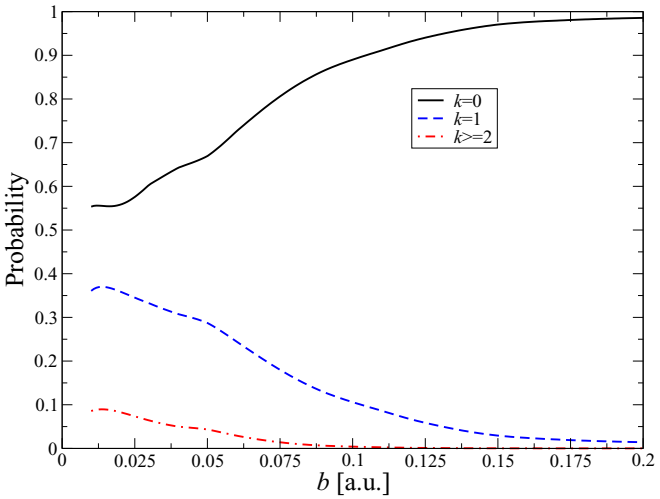

FIG. 6. (Color online) The probabilities of the Bi k-L_3-shell ($2p_{3/2}$) electronic population in the Xe-Bi^{83+} collision as functions of the impact parameter b.

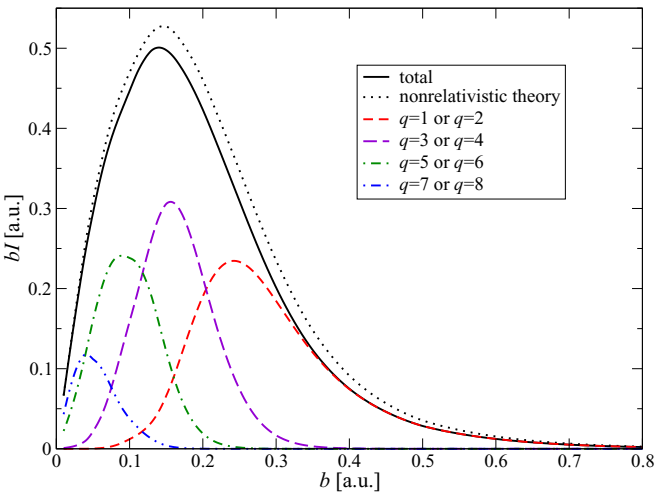

FIG. 8. (Color online) The total and q intensities I of the Xe L-shell-vacancy production weighted by the impact parameter in the Xe-Bi^{83+} collision as functions of the impact parameter b. The dotted line indicates the total results of the nonrelativistic calculations.

TABLE I. Cross sections σ (10^{-14} cm^2) of the x-ray radiation processes for the Xe-Bi^{83+} collision.

Process	(Xe, K)	(Xe, L)	(Bi, K_{α_1}) ($2p_{3/2}$-$1s$)	(Bi, K'_{α_2}) ($2p_{1/2}$-$1s$)	(Bi, K''_{α_2}) ($2s$-$1s$)
σ of the x-ray radiation	47(3)	200(25)	20(6)	13(4)	26(10)
Nonrelativistic theory (for collisional dynamics)	50	218	31	20	24

we evaluated the corresponding values in the nonrelativistic limit ($c \to \infty$) by performing the same computing procedure, but with a 1000 times increased value of the speed of light (in atomic units). This modification allows us to carry out the nonrelativistic evaluation of the electronic collisional dynamics. In the figures the obtained nonrelativistic data are indicated by the dotted lines. In Fig. 8, the contributions from the q-L-shell-vacancy production processes to the total intensity are also presented. For the evaluation of $I_K^{\rm rad}$ and $I_L^{\rm rad}$ the values of the fluorescence yield $P^{\rm rad}(K) = 0.89(1)$ and $P^{\rm rad}(L) = 0.09(1)$ are taken from Refs. [34,35]. These values are based on the experimental and theoretical analysis.

We note that at the values of the impact parameter, where the integral (12) is assembled (see Fig. 7), the L shell is almost empty (see Fig. 2). It decreases the probability of the K shell filling by the Auger decay and, therefore, the value of $P^{\rm rad}(K)$ is underestimated. Thus, it is reasonable to expect a little bit underestimated (up to 5%) the value of $I_K^{\rm rad}$. The fluorescence yield coefficient for the L shell is actually individual for each L subshell (L_1, L_2, L_3). Here we use the average value of the coefficient over the subshells. With a high probability (about 70%) a vacancy in the K shell leads to a vacancy in the L shell. This is in accordance with the experimental data for the relative intensities of the K_α and K_β x-ray lines [24]. But the intensity of the K-shell-vacancy production does not exceed 2% of the L-shell one. That is why we neglect this contribution to the L-shell-vacancy production processes. The final values of the radiative intensities per collision or the total cross sections of the radiation processes are presented in Table I.

According to our study (see Sec. III A), the bismuth ion captures just a few electrons. Due to the small electron number and the rather large nuclear charge number, the probability of the Auger processes in the bismuth ion is negligible. In accordance with the values of the radiative transition probabilities [36], the electrons de-excite from the L_1, L_2, L_3, M, N, and other shells to the K shell in the following order: first from the L_2 and L_3 shells, then from the M, N, and higher shells and, finally, from the L_1 shell. We also note that the probability to find two K-shell vacancies exceeds 0.8 for the impact parameter larger than 0.025 a.u., where the K_α radiation cross section is assembled (see below). But the maximum of the total probability to capture more than two electrons to the L, M, and N shells is less than 0.2. That is why we assume that surely almost all the L_2-, L_3-, and even the majority of the L_1-shell electrons de-excite radiatively to the K shell. Moreover, since the probability of the radiative de-excitation from the $np_{1/2}$ and $np_{3/2}$ states to the $1s$ state by cascades is at least five times less than by the direct transition [36] and the population of the M, N, and higher shells is low, the cascades processes leading to the K_α radiation can be neglected to a good accuracy. In order to obtain the intensities of the $2p_{3/2}$-$1s$ (K_{α_1}), $2p_{1/2}$-$1s$ (K'_{α_2}), and $2s$-$1s$ (K''_{α_2}) lines, we calculate the probabilities P_f of all possible atomic state configuration with n_K, n_{L_1}, n_{L_2}, n_{L_3} electrons in the K, L_1, L_2, L_3 shells, correspondingly. Then we evaluate the radiative de-excitation probabilities with

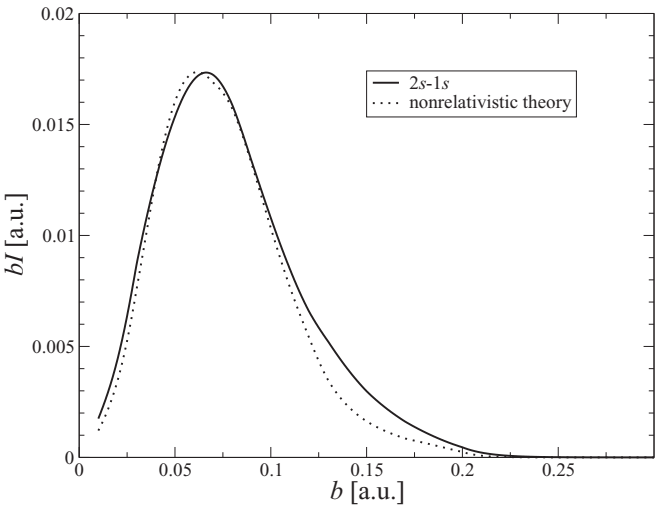

FIG. 9. The intensity I of the Bi K''_{α_2} radiation weighted by the impact parameter in the Xe-Bi^{83+} collision as a function of the impact parameter b. The dotted line indicates the results of the nonrelativistic calculations.

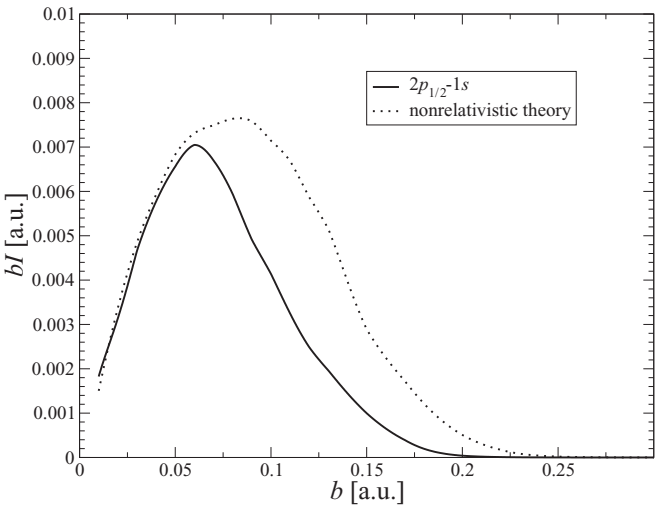

FIG. 10. The intensity I of the Bi K'_{α_2} radiation weighted by the impact parameter in the Xe-Bi^{83+} collision as a function of the impact parameter b. The dotted line indicates the results of the nonrelativistic calculations.

TABLE II. Relative intensities of the x-ray radiation for the Xe-Bi^{83+} collision.

	(Xe, L)/(Xe, K)	(Bi, K_{α_1})/(Xe, K)	(Bi, K_{α_2})/(Xe, K)
Theory (this work)	4.2(6)	0.43(14)	0.83(30)
Experiment [24]	3.6(2)	0.59(3)	0.69(3)

m K_{α_1}, K'_{α_2} or K''_{α_2} photons $P^{\rm rad}_{m,K_{\alpha_i}}(f)$ in accordance with the radiative transition probabilities from the L_i to K shell for hydrogenlike bismuth A_{L_i} ($A_{L_1}/A_{L_2} = 0$, $A_{L_1}/A_{L_3} = 0$, $A_{L_2}/A_{L_3} = 31/27$) [36]. Finally, the relative x-ray radiation intensities are given by $I^{\rm rad}_{K_{\alpha_i}}(b) = \sum_f m P^{\rm rad}_{m,K_{\alpha_i}}(f) P_f(b)$. The results of the calculations of $I^{\rm rad}_{K''_{\alpha_2}}(b)$, $I^{\rm rad}_{K'_{\alpha_2}}(b)$, and $I^{\rm rad}_{K_{\alpha_1}}(b)$ weighted by the impact parameter are presented in Figs. 9, 10, and 11, respectively. In the figures, the obtained nonrelativistic data are indicated by the dotted lines. We note a rather strong influence of the relativistic effects on the intensities of the K_{α_1} and K'_{α_2} (but not K''_{α_2}) lines.

The final values of the radiative intensities per collision or the total cross sections of the radiation processes are collected in Table I. The uncertainties of the obtained data, being estimated rather conservatively, account for the errors due to both collision calculation and post-collisional analysis. For bismuth the uncertainty is much larger than for xenon. This is caused by the use of the moving orbitals and the more difficult post-collisional analysis for the bismuth ion. The relativistic effects are really large and reach 50% for the K_{α_1} and K'_{α_2} intensities. We note that the nonrelativistic data are obtained within the nonrelativistic calculation of the electronic collisional dynamics, but with using the relativistic values of the fluorescence yields and transition coefficients for the post-collisional analysis.

The relative intensities and comparison with the experiment [24] are presented in Table II. It can be seen that the theoretical results are in reasonable agreement with the experimental ones. Some underestimation of the theoretical intensities for the bismuth K_{α_1} emission might be explained by disregarding the cascade radiation processes from the higher-excited bismuth shells and a possible anisotropy of the K_{α_1} radiation (see, e.g., Ref. [37]; the x-ray spectrum in the experiment was recorded by a detector mounted at the observation angle of 150 deg). In the same way, the somewhat smaller experimental intensity of the Xenon L radiation might possibly be due to the transitions from high n states, which cannot be fully resolved in the experiment. We expect that the theoretical results can be further improved by the calculations with a larger basis set and by including higher shells of bismuth to the post-collisional analysis.

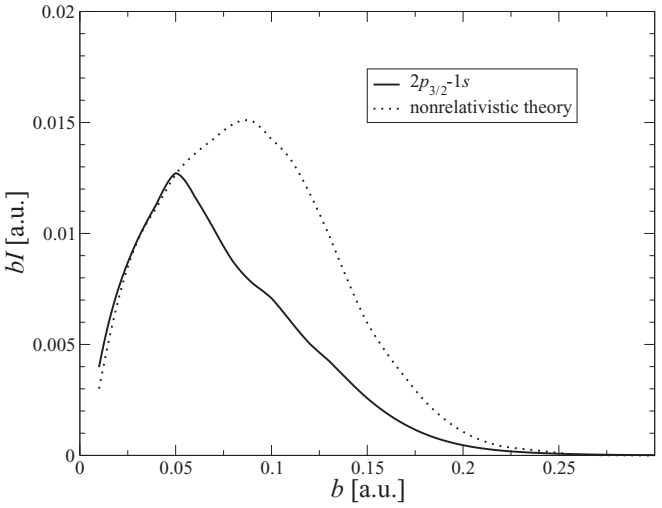

FIG. 11. The intensity I of the Bi K_{α_1} radiation weighted by the impact parameter in the Xe-Bi^{83+} collision as a function of the impact parameter b. The dotted line indicates the results of the nonrelativistic calculations.

IV. CONCLUSION

We have evaluated the post-collisional x-ray emission in the Bi^{83+} - Xe collision at the projectile energy 70 MeV/u, treating separately the collisional and post-collisional processes. The many-electron excitation, ionization, and charge-transfer probabilities were calculated within the independent particle model using the coupled-channel approach with the atomiclike Dirac-Fock-Sturm orbitals. The inner-shell atom and ion processes were comprehensively studied and the corresponding probabilities were presented as functions of the impact parameter. The analysis of the post-collisional processes leading to the x-ray emission was based on the fluorescence yields, the radiation, and Auger decay rates. It allows us to derive the x-ray radiation intensities and compare them with the related experimental data. The higher accuracy of the theoretical predictions for the xenon (target) x-ray radiation intensities is caused by the easier decay analysis and the use of the nonmoving atomic orbitals. The obtained results are in reasonable agreement with the experimental data.

The theoretical study demonstrates a very significant role of the relativistic effects, up to 50% for the bismuth x-ray radiation intensities. Thus, investigations of heavy highly charged ion-atom collisions seem very promising for tests of relativistic and QED effects in scattering processes.

ACKNOWLEDGMENTS

This work was supported by RFBR (Grants No. 14-02-31418, No. 13-02-00630, No. 12-03-01140-a, and No. 14-02-00241), GSI, and SPbSU (Grants No. 11.50.1607.2013, No. 11.38.269.2014, and No. 11.38.261.2014). Y.S.K. acknowledges financial support from the Helmholtz Association and SAEC Rosatom. The work of A.G. was supported by the Alliance Program of the Helmholtz Association (HA216/EMMI).

[1] R. Schuch, G. Nolte, H. Schmidt-Böcking, and W. Lichtenberg, Phys. Rev. Lett. **43**, 1104 (1979).

[2] D. Liesen, P. Armbruster, F. Bosch, S. Hagmann, P. H. Mokler, H. J. Wollersheim, H. Schmidt-Böcking, R. Schuch, and J. B. Wilhelmy, Phys. Rev. Lett. **44**, 983 (1980).

[3] S. Hagmann, C. L. Cocke, J. R. Macdonald, P. Richard, H. Schmidt-Böcking, and R. Schuch, Phys. Rev. A **25**, 1918 (1982).

[4] J. A. Tanis, E. M. Bernstein, W. G. Graham, M. Clark, S. M. Shafroth, B. M. Johnson, K. W. Jones, and M. Meron, Phys. Rev. Lett. **49**, 1325 (1982).

[5] P. L. Pepmiller, P. Richard, J. Newcomb, J. Hall, and T. R. Dillingham, Phys. Rev. A **31**, 734 (1985).

[6] W. Fritsch and C. D. Lin, Phys. Rep. **202**, 1 (1991).

[7] M. Barat and P. Roncin, J. Phys. B **25**, 2205 (1992).

[8] B. H. Bransden and M. R. C. McDowell, *Charge Exchange and the Theory of Ion-Atom Collisions* (Oxford University Press, New York, 1992).

[9] P. Kürpick, W.-D. Sepp, and B. Fricke, Phys. Rev. A **51**, 3693 (1995).

[10] H. J. Lüdde, A. Henne, T. Kirchner, and R. M. Dreizler, J. Phys. B **29**, 4423 (1996).

[11] A. Arnau, F. Aumayr, P. M. Echenique, M. Grether, W. Heiland, J. Limburg, R. Morgenstern, P. Roncin, S. Schippers, R. Schuch, N. Stolterfoht, P. Varga, T. J. M. Zouros, and H. P. Winter, Surf. Sci. Rep. **27**, 117 (1997).

[12] S. Otranto, R. E. Olson, and P. Beiersdorfer, Phys. Rev. A **73**, 022723 (2006).

[13] K. Dennerl, Space Sci. Rev. **157**, 57 (2010).

[14] I. Yu. Tolstikhina and V. P. Shevelko, Phys.-Usp. **56**, 213 (2013).

[15] J. Eichler and W. E. Meyerhof, *Relativistic Atomic Collisions* (Academic Press, New York, 1995).

[16] V. M. Shabaev, Phys. Rep. **356**, 119 (2002).

[17] J. Eichler and T. Stöhlker, Phys. Rep. **439**, 1 (2007).

[18] W. Greiner, B. Müller, and J. Rafelski, *Quantum Electrodynamics of Strong Fields* (Springer-Verlag, Berlin, 1985).

[19] http://www.gsi.de/en/research/fair.htm.

[20] http://www.gsi.de/sparc.

[21] M. Lestinnsky *et al.*, CRYRING@ESR: A Study Group Report (unpublished).

[22] S. Hagmann, Ch. Kozhuharov, Th. Stöhlker, V. Shabayev, I. Tupitsyn, D. Fischer, R. Grisenti, A. Gumberidze, F. Bosch, D. Liesen, U. Spillmann, R. Märtin, R. Reuschl, M. Trassinelli, S. Trotsenko, G. Weber, P.-M. Hillenbrand, N. Petridis, R. Dubois, D. Thorn, R. Dörner, D. Winter, H. Rothard, J. Ullrich, R. Moshammer, and E. de Filippo (unpublished).

[23] A. Gumberidze, R. D. DuBois, F. Bosh, R. Grisenti, T. Gross, S. Hagmann, M. Hegewald, P. Indelicato, C. Kozhuharov, D. Liesen, R. Märtin, R. Reuschl, M. Schwemlein, U. Spillmann, Th. Stöhlker, D. Thorn, M. Trassinelli, S. Trotsenko, A. Warczak, G. Weber, D. F. A. Winters, and N. Winters (unpublished).

[24] A. Gumberidze, R. D. DuBois, C. Kozhuharov, C. Brandau, M. Schwemlein, K.-H. Blumenhagen, A. Bräuning-Demian, W. Chen, R. Grisenti, S. Hagmann, P. Indelicato, M. Lestinsky, Y. Litvinov, R. Märtin, N. Petridis, R. Reuschl, U. Spillmann, S. Trotsenko, P. Verma, G. Weber, W. Wen, D. F. A. Winters, N. Winters, and Th. Stöhlker, GSI Sci. Rep. 365 (2011).

[25] I. I. Tupitsyn, Y. S. Kozhedub, V. M. Shabaev, A. I. Bondarev, G. B. Deyneka, I. A. Maltsev, S. Hagmann, G. Plunien, and Th. Stöhlker, Phys. Rev. A **85**, 032712 (2012).

[26] Y. S. Kozhedub, I. I. Tupitsyn, V. M. Shabaev, S. Hagmann, G. Plunien, and Th. Stöhlker, Phys. Scr., T **156**, 014053 (2013).

[27] J. P. Perdew and A. Zunger, Phys. Rev. B **23**, 5048 (1981).

[28] V. F. Brattsev, G. B. Deyneka, and I. I. Tupitsyn, Bull. Acad. Sci. USSR, Phys. Ser. **41**, 173 (1977).

[29] I. I. Tupitsyn, Y. S. Kozhedub, V. M. Shabaev, G. B. Deyneka, S. Hagmann, C. Kozhuharov, G. Plunien, and Th. Stöhlker, Phys. Rev. A **82**, 042701 (2010).

[30] J. Crank and P. Nicholson, Proc. Cambridge Philos. Soc. **43**, 50 (1947).

[31] M. D. Feit, J. A. Fleck, Jr., and A. Steiger, J. Comput. Phys. **47**, 412 (1982).

[32] H. J. Lüdde and R. M. Dreizler, J. Phys. B **18**, 107 (1985).

[33] P. Kürpick and H. J. Lüdde, Comput. Phys. Commun. **75**, 127 (1993).

[34] R. E. Van Grieken and A. A. Markowicz (eds.), *Handbook of X-Ray Spectrometry* (Marcel Dekker, New York/Basel, 2002).

[35] J. H. Hubbell, P. N. Trehan, N. Singh, B. Chand, D. Mehta, M. L. Garg, R. R. Garg, S. Singh, and S. Puri, J. Phys. Chem. Ref. Data A **23**, 339 (1994).

[36] O. Jitrik and C. F. Bungea, J. Phys. Chem. Ref. Data **33**, 1059 (2004).

[37] A. Surzhykov, S. Fritzsche, A. Gumberidze, and Th. Stöhlker, Phys. Rev. Lett. **88**, 153001 (2002).